

Influence of adhesive bond layer on power and energy transduction efficiency of piezo-impedance transducer

Journal of Intelligent Material Systems and Structures

1–13

© The Author(s) 2014

Reprints and permissions:

sagepub.co.uk/journalsPermissions.nav

DOI: 10.1177/1045389X14523858

jim.sagepub.com



Sumedha Moharana^{1,2} and Suresh Bhalla¹

Abstract

This article deals with the analysis of the power consumption in the piezoelectric ceramic patch of lead zirconate titanate and the losses arising from the adhesive bonding with the host structure. When a lead zirconate titanate patch is utilized as an impedance transducer in the electromechanical impedance technique, it acts both as a sensor and as an actuator (dual effect) for the range of frequency. Power consumption occurs in two forms. First part of the energy is used to actuate the lead zirconate titanate patch and produce deformations. The other part of the energy is dissipated within the piezo-mechanical system due to the internal mechanical loss and the associated heat generation. The determination of the power consumption characteristics for an active piezo-system is very important for designing an efficient intelligent structure with optimized mass and energy combination. Adhesive bond itself acts as an added stiffness, mass and damper and plays an important role in mechanical and electrical energy conversion. Hence, a detailed investigation is needed to characterize the power consumption and energy issues associated with bond layer driven by lead zirconate titanate patch, which is the main aim of this article.

Keywords

Electromechanical admittance, active power, dissipative power, power factor, electromechanical coupling coefficient, loss factor

Introduction

Integrated induced strain transducers provide the necessary energy for an intelligent system to respond adaptively to an internal or an external stimulus. The transducer power consumption as well as the energy transfer from the transducer to the host structure and vice versa is an important issue in the application and design of intelligent material systems and structures. In the electromechanical impedance (EMI) technique for structural health monitoring (SHM), the piezoelectric ceramic patch lead zirconate titanate (PZT) couples the electrical and the mechanical parameters simultaneously and acts as both sensor and actuator. Here, although actuation is part of the mechanical interaction, the forces involved are very small. In either case, for a system with integrated PZT patches, the power consumed by the patches consists of two parts: the energy used to drive the system, which is dissipated in terms of heat (as a result of the structural damping), and energy dissipated by the PZT patches themselves because of their dielectric loss and internal structural damping (Liang et al., 1995).

The power consumption is related to the designated function of the piezo-system, that is, whether it is used for shape control, health monitoring, vibration or acoustic control, as well as the associated electronic systems, including the power supply itself. In the treatment of this article, the power supply system is not included in the coupled electromechanical analysis by assuming that the power supply system can always satisfy the current needs of the actuator, in line with the assumption of Liang et al. (1994). In vibration control, the energy supplied to the PZT patch is absorbed by the structural damping of the mechanical system and the internal damping and the dielectric loss of the PZT

¹Department of Civil Engineering, Indian Institute of Technology Delhi, New Delhi, India

²Department of Civil Engineering, School of Engineering, Shiv Nadar University, Dadri, UP, India. (Formerly Research Scholar, Department of Civil Engineering, IIT Delhi)

Corresponding author:

Suresh Bhalla, Department of Civil Engineering, Indian Institute of Technology Delhi, Hauz Khas, New Delhi 110016, India.
Email: sbhalla@civil.iitd.ac.in

actuator. For acoustic control, most of the electrical and the mechanical energy is used to radiate sound. In shape control, all the system energy is transferred from the reactive electric energy into the reactive mechanical energy (strain energy) but still stored in the electromechanical system. In SHM (especially the EMI technique), all the electrical reactive energy is converted into the mechanical reactive energy and vice versa because of the dual piezoelectric effect.

As a matter of fact, this issue was duly recognized during the early development and implementation of PZT patches. In the beginning, several static modelling techniques were developed to determine the equivalent static forces or moments (Bailey and Hubbard, 1985; Crawley and De Luis, 1987; Dirmitriadis et al., 1989; Wang and Rogers, 1991). The quasi-static analysis using the static model is not very accurate because the active forces originated by the PZT patches are harmonic in nature. The dynamic interaction between the host structure and the PZT patch exists and affects the performance of both the structure and the patch. Later on, the impedance-based analytical model developed by Liang and co-workers provided a better modelling of the dynamic characterization of PZT element-driven systems (Bhalla et al., 2009; Bhalla and Soh, 2004(b,c); Liang et al., 1994; Zhou et al., 1996). The frequency-dependent force output behaviour is accurately predicted by the impedance approach.

The bonding effect on the electromechanical admittance output has been modelled by various researchers through numerous analytical models (Bhalla et al., 2009; Bhalla and Soh, 2004(a); Dugnani, 2009; Giurgiutiu and Santoni-Bottai, 2009; Han et al., 2008; Huang et al., 2010; Ong et al., 2002; Park et al., 2008; Tinoco et al., 2010; Xu and Liu, 2002; Yu et al., 2010) supplemented with experimental verification. All the studies concluded that the bond layer has significant impact on coupled admittance signature. Several numerical investigations on shear lag effect (Giurgiutiu and Santoni-Bottai, 2006; Jin and Wang, 2011; Liu and Giurgiutiu, 2007; Yang et al., 2008, 2011; Zhang et al., 2011) have been reported to accommodate the bonding effect. However, the effect of the bond layer on energy transduction characteristics has not been studied.

The designers of the engineering and space structures are also concerned with how efficiently a PZT patch acts as a transducer to transform the electrical energy into the mechanical energy. Liang et al. (1996) analysed the power components to interpret the usage of the electromechanical properties of piezo-transducers in various applications. They suggested a power factor, defined as the ratio of the dissipative mechanical power in the system to the total electrical power supplied to the patch. This concept was used to optimize the location of the actuator (Liang et al., 1995). Stein et al. (1994) investigated the power consumption of a PZT actuator integrated with an underwater structure that

radiated sound and evaluated the power requirements in active acoustic control.

The influence of various loss parameters on the system power factor and the system power requirement was studied in detail by Zhou et al. (1996), who extended the impedance model to two-dimensional (2D). Lin and Giurgiutiu (2012) developed a one-dimensional (1D) guided axial and flexural wave-based predictive model for computing the power and the energy transduction between structurally guided waves and piezo-wafer active sensor (PWAS) through closed-form analytical expressions. The power and energy analyses for single PWAS transmitter, single PWAS receiver and a complete PWAS in pitch-catch set-up were carried out. Frequency response functions were derived for voltage, current, complex power, active power and so on. They concluded that a judicious combination of PWAS size, structural thickness and excitation frequency can ensure optimal energy transduction and coupling with the ultrasonic-guided waves travelling in the structure. However, they considered only 1D guided axial and flexural waves for the analysis.

The above literature shows that although a number of studies have been conducted for power and energy efficiency, none have explicitly considered the influence of the bond layer. The recent analytical developments show that bond layer has strong influence on piezo-structure system. Therefore, the next section aims to examine the power consumption and energy efficiency related to the EMI technique through the continuum-based piezo-elastodynamic model (Moharana and Bhalla, 2014) considering all piezo-mechanical properties of the adhesive bond in a continuous manner along the bonding area. Hence, taking the advantage of accuracy and simplicity of the continuum model, the power factor and energy conversion efficiency ratio have been redefined, along with the fact that the shear stress and inertia effect are considered simultaneously. A modified coupling coefficient has also been proposed based on continuum piezo-bond-structure model.

Continuum-based electromechanical model for modelling the bond effect

The governing dynamic shear lag equation (Bhalla and Soh, 2004a) for an infinitesimal element of PZT patch, shown in Figure 1, can be written as

$$\tau w dx + (dm)\ddot{u}_p = \frac{\partial T_1}{\partial x} h w dx \quad (1)$$

where u_p is the displacement in the PZT patch, dm is the mass of the infinitesimal element, τ is the interfacial shear stress, T_1 is the axial stress in the PZT patch, w is the width of the patch, l is the half length and h is the thickness. Bhalla and Soh (2004a) had simplified equation (1) by ignoring the inertia term $(dm)\ddot{u}_p$. However,

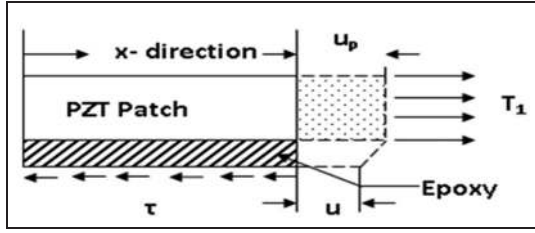


Figure 1. Deformation in bond layer and PZT patch. PZT: lead zirconate titanate.

recently, Bhalla and Moharana (2013) in their new modelling approach termed as ‘refined model’, solved equation (1) duly considering both inertia term and shear stress simultaneously to derive an accurate and more realistic governing equation, expressed as

$$u'''' + \bar{p}u'' - \bar{\alpha}qu' + (1 - \bar{\alpha})\bar{p}qu = 0 \quad (2)$$

where \bar{p} and q are the shear lag parameters, $\bar{\alpha}$ is the inertia parameter (Bhalla and Moharana, 2013) and u is the displacement of structure, which is ultimately utilized at the edge of the PZT patch relative to the patch’s displacement to evaluate the equivalent mechanical impedance of the structure-bond layer combined system, given by

$$Z_{eq} = Z_s \frac{u(x=l)}{u_p(x=l)} \quad (3)$$

where Z_{eq} and Z_s are the equivalent mechanical impedance (including bond effect) and structural impedance (without bond effect), respectively, and $u_{(x=l)}$ and $u_{p(x=l)}$ are the tip displacements of the host structure and the PZT patch, respectively.

The final expression of electromechanical admittance (\bar{Y}) based on the above treatment can be written for a square PZT as

$$\bar{Y} = \frac{\bar{I}}{\bar{V}} = G + Bj = 4\omega j \frac{l^2}{h_p} \left[\frac{\bar{\epsilon}_{33}^T}{\epsilon_{33}^T} - \frac{2d_{31}^2 \bar{Y}^E}{(1-\nu)} + \frac{2d_{31}^2 \bar{Y}^E}{(1-\nu)} \left(\frac{Z_{a,eff}}{Z_{s,eff} + Z_{a,eff}} \right) \bar{T} \right] \quad (4)$$

where ω is the angular frequency, l is the half length, h_p is the thickness of the PZT patch, $\frac{\bar{\epsilon}_{33}^T}{\epsilon_{33}^T} = \epsilon_{33}(1 - \delta j)$ is the complex piezoelectric permittivity (δ being the dielectric loss factor), $\bar{Y}^E = Y^E(1 + \eta j)$ is the complex Young’s modulus (η being the mechanical loss factor), Z_a is the mechanical impedance of the PZT patch, $Z_{s,eff}$ is the effective mechanical impedance of the host structure and \bar{T} is the tangent ratio term (Bhalla and Soh, 2004(b,c)). The superscripts E and T denote that the quantity is considered constant at electric field and stress, respectively. The main limitation of the above refined model is that the interaction between the structure and patch is restricted at the ends of the patch

only. shear lag model, a new continuum-based admittance has been derived by Moharana and Bhalla (2014) rigorously considering shear transfer phenomena through the adhesive layer continuously and simultaneously throughout the bond area, eliminating the computation of the equivalent structural impedance ($Z_{s,eq}$), at ($x=l$) only (see equation (3)). In this approach, the dynamic shear lag equilibrium equation was solved for displacement (u) and strains (S_x and S_y) as

$$u = A_1 e^{\lambda_1 x} + A_2 e^{\lambda_2 x} + A_3 e^{\lambda_3 x} \quad (5)$$

where λ_1 , λ_2 and λ_3 are the three complex roots of the governing differential equation and A_1 , A_2 and A_3 are the three unknown coefficients of the solution. S_x and S_y can be expressed as

$$S_1 = u'_{px} = \left(1 + \frac{\lambda_1}{\bar{p}_{eff}} \right) \lambda_1 e^{\lambda_1 x} A_1 + \left(1 + \frac{\lambda_2}{\bar{p}_{eff}} \right) \lambda_2 e^{\lambda_2 x} A_2 + \left(1 + \frac{\lambda_3}{\bar{p}_{eff}} \right) \lambda_3 e^{\lambda_3 x} A_3 \quad (6a)$$

$$S_2 = u'_{py} = \left(1 + \frac{\lambda_1}{\bar{p}_{eff}} \right) \lambda_1 e^{\lambda_1 y} A_1 + \left(1 + \frac{\lambda_2}{\bar{p}_{eff}} \right) \lambda_2 e^{\lambda_2 y} A_2 + \left(1 + \frac{\lambda_3}{\bar{p}_{eff}} \right) \lambda_3 e^{\lambda_3 y} A_3 \quad (6b)$$

where \bar{p}_{eff} is the shear lag parameter for 2D case, evaluated as (Bhalla and Moharana, 2013)

$$\bar{p}_{eff} = -\frac{2l\bar{G}_s(1+\nu)}{Z_{s,eff}j\omega h_s} \quad (7)$$

where h_s is the bond thickness.

In the continuum approach, the electric current is expressed as

$$\bar{I} = 4j\omega \bar{V} \frac{l^2}{h_p} \left[\frac{\bar{\epsilon}_{33}^T}{\epsilon_{33}^T} - \frac{2d_{31}^2 \bar{Y}^E}{(1-\nu)} \right] + j\omega d_{31} \frac{\bar{Y}^E}{(1-\nu)} \iint_A (S_1 + S_2) dx dy \quad (8)$$

The second integration is carried out in a continuous manner using equations (6a) and (6b) (in contrast to conventional approach). The coefficients A_1 , A_2 and A_3 can be determined from the imposed boundary condition leading to the following final expression

$$\bar{Y} = \frac{\bar{I}}{\bar{V}} = 4j\omega \frac{l^2}{h_p} \left[\frac{\bar{\epsilon}_{33}^T}{\epsilon_{33}^T} - \frac{2d_{31}^2 \bar{Y}^E}{(1-\nu)} \right] - \frac{8lj\omega d_{31} \bar{Y}^E}{(1-\nu)\bar{V}} [U_{con}] \quad (9)$$

where U_{con} denotes continuum displacement generated by rigorous integration.

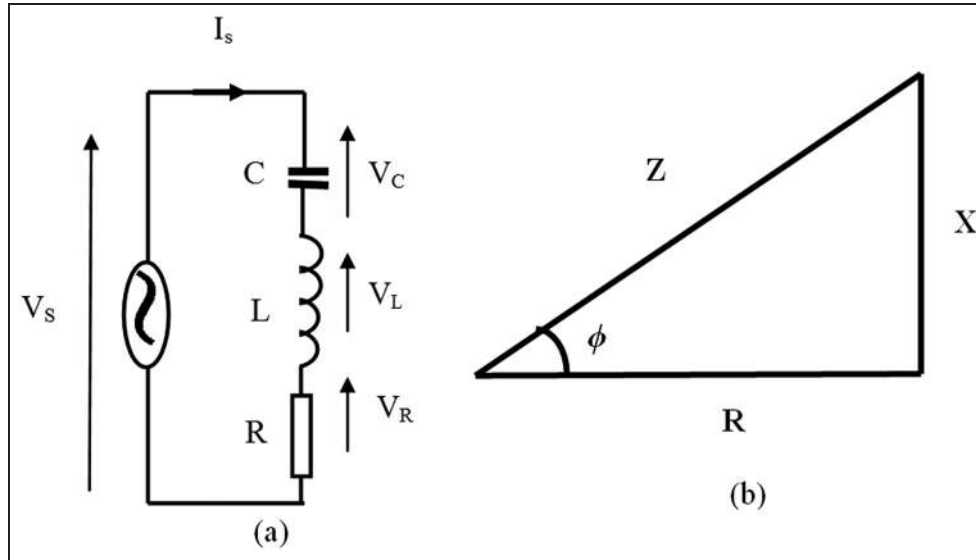


Figure 2. (a) Series combination of LCR circuit (the inductance (L), the resistance (R) and the capacitance (C)) and (b) impedance triangle for LCR circuit.

Electrical impedance and power triangle

In general, the impedance term refers to electrical load, which acts opposite to the electromotive force. The combined effect of the resistance (R), inductive reactance (X_L) and capacitive reactance (X_C) in an AC circuit under an alternating voltage source operating at a frequency f is shown in Figure 2(a). The impedance triangle for the circuit in series is shown in Figure 2(b) (Watkins and Kitcher, 2006). The vector representations of current and voltage for piezo-capacitive circuit and electrical power triangle have been shown in Figure 3. Making equivalence of the two similar triangles (Figures 2(b) and 3(b)), we can obtain the following relationships between electrical power and electrical impedance

$$\bar{Z}_e = R + Xj \quad (10)$$

Equation (10) can be rewritten in the admittance form as

$$\bar{Y} = G + Bj = \frac{1}{\bar{Z}_e} = \frac{1}{R + Xj} \quad (11)$$

On simplification of equation (11), the conductance and susceptance terms can be expressed in terms of R and X as

$$G = \frac{R}{(R^2 + X^2)} \quad (12a)$$

$$B = \frac{-X}{(R^2 + X^2)} \quad (12b)$$

The phase angle between the voltage and current can be determined as

$$\tan \phi = \frac{X}{R} = \left(-\frac{B}{G} \right) \quad (13)$$

The power factor of impedance circuit can be defined as

$$\cos \phi = \frac{R}{|Z_e|} = \frac{G}{|Y|} \quad (14)$$

As evident from Figure 3, the impedance and power triangles of impedance are similar. We can thus conclude that

$$\frac{W_D}{R} = \frac{W_R}{X} = \frac{W_A}{Z_e} \quad (15)$$

where W_A , W_D and W_R are the apparent, active and reactive power components, respectively. The sign of angle ϕ must be accounted, for instance, if

- (1) $\phi > 0 \Rightarrow 0 < W_R < 0$ and $X > 0$ (inductive impedance)
- (2) $\phi < 0 \Rightarrow 0 < W_R < 0$ and $X < 0$ (capacitive impedance)

The next section deals with computation of the above quantities for a piezo-patch in the EMI technique.

Electrical power consumption in piezo-impedance transducer

Apparent power

The apparent power (V·A), W_A , in terms of admittance function can be defined as

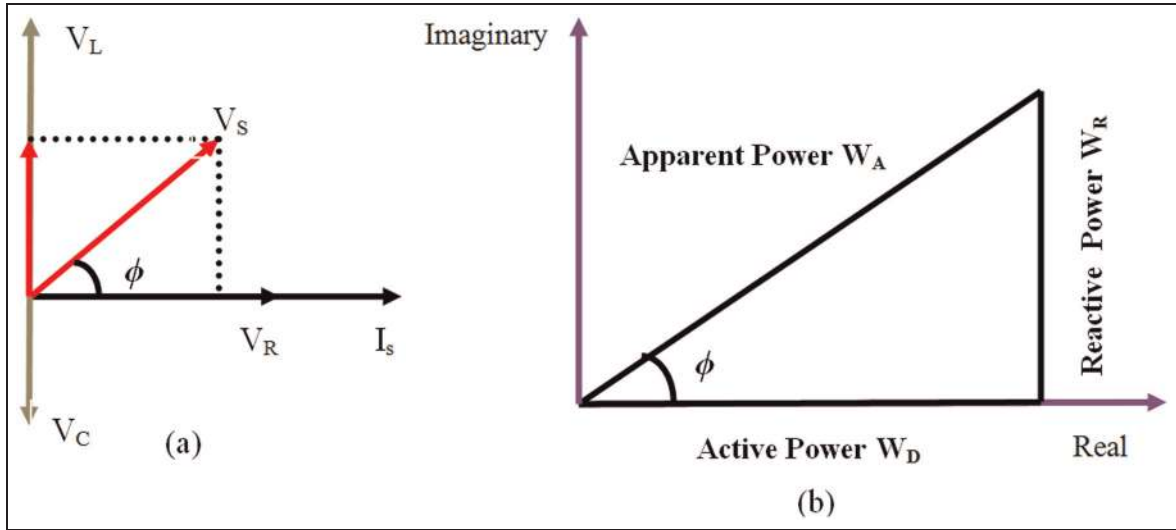


Figure 3. (a) Vector representation of voltage and current on complex plane and (b) power triangle.

$$P_{\text{apparent}} = W_A = VI = \frac{V_0^2}{2} |Y| \quad (16)$$

where $|Y|$ is the absolute value of the admittance signature and V and I are the root mean square values of the corresponding quantity. V_0 is the peak excitation voltage given by $V_0 = \sqrt{2}V_{\text{rms}}$.

The apparent power is the quantity of power initially applied to the PZT patch to induce the strain deformation. As we know, a piezo-patch behaves as a capacitor, the induced displacement is proportional to the stored charge, and hence, the apparent power is greater than the active power.

Active power

The active or the dissipative power (W) W_D can be defined as

$$P_{\text{active}} = W_D = W_A \cos \phi = \frac{V_0^2}{2} \text{Re}(\bar{Y}) \quad (17)$$

The active power is a measurement of the rate at which the electricity performs works such as producing heat, light or mechanical energy. The amount of power actually consumed in the piezo-system and dissipated as the dielectric and the structural losses results in the active or real power. The piezo-capacitance causes the phase lag between the current and the voltage. The active power is the power dissipated in the piezo-system in the form of heat, sound and mechanical deformations and reflects itself in system through acoustic impedance and structural damping. Some part of power may be lost due to internal structural damping of structure, internal damping (η) and the dielectric loss of piezo-patch (δ). The authors have termed all these losses as mechanical losses collectively.

Reactive power

The vector difference between the apparent and active power is called reactive power. From Figure 3, the reactive power, W_R can be mathematically expressed as

$$P_{\text{reactive}} = W_R = W_A \sin \phi = \frac{V_0^2}{2} \text{Im}(\bar{Y}) \quad (18)$$

The energy stored in the capacitive PZT patch undergoes periodical reversal. Some of part of the energy is temporarily stored by itself due its capacitive nature. Due to this reason, the reactive power of the piezo-patch continuously flows within it, similar to the strain energy stored in a spring-mass system.

The relation between the apparent power, active power and reactive power can be written as

$$P_{\text{apparent}}^2 = P_{\text{active}}^2 + P_{\text{reactive}}^2 \quad (19)$$

In order to maintain the constant voltage supply to piezoelectric system, one needs to ensure meeting a minimum power requirement, which is called the power rating, and below which, the PZT patch will cease to operate. This is expressed in terms of the maximum absolute admittance as

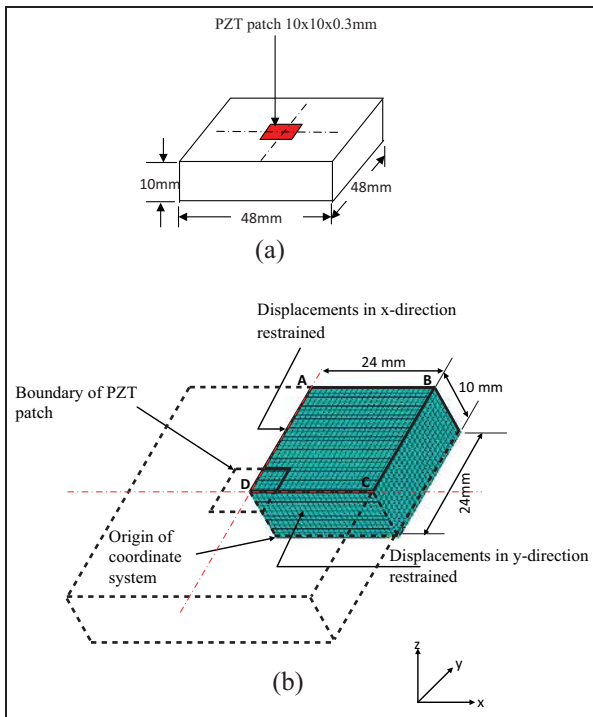
$$P_{\text{rating}} = W_{\text{rating}} = \frac{V_0^2}{2} \max(|\bar{Y}|) \quad (20)$$

The influence of the adhesive bond layer on the electrical power components of piezo-structural interaction system comprising an aluminium block and a PZT patch shown in Figure 4, with material parameters listed in Table 1, is analysed in this section. Continuum modelling approach (Moharana and Bhalla, 2014) has been employed. Comparison is made with perfect bonding (no adhesive bonding) in order to highlight the

Table 1. Parameters of PZT patch, aluminium block and adhesive bond.

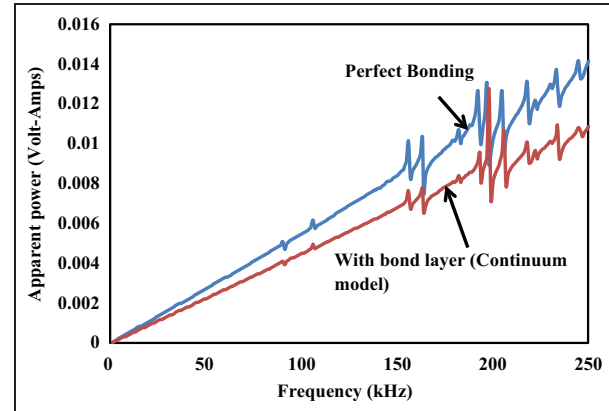
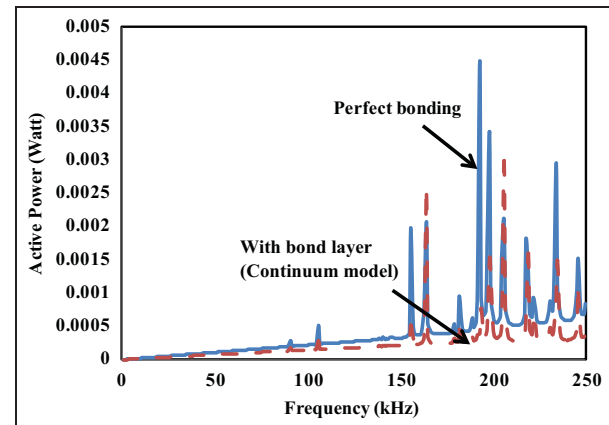
Material	Physical parameter	Value
PZT patch	Electric permittivity $\overline{\epsilon}_{33}^T$ (F/m)	1.7785×10^{-8}
	Peak correction factor (C_1, C_2)	0.898
	$k = \frac{2d_{31}^2 Y^E}{(1-\nu)}$ (N/V ²)	5.35×10^{-9}
	Mechanical loss factor η	0.0325
Aluminium block	Dielectric loss factor δ	0.0224
	Young's modulus (GPa)	68.95
	Density (kg/m ³)	2715
	Poisson's ratio	0.33
	Rayleigh damping coefficients	
Adhesive	α	0
	β	3×10^{-9}
	Mechanical loss factor η'	0.1

PZT: lead zirconate titanate.

**Figure 4.** Comparison of refined model with previous model: (a) aluminium block structure and (b) finite element model of a quarter of structure.

PZT: lead zirconate titanate.

effect of bonding. Finite element simulation (Bhalla and Moharana, 2013) is used to obtain $Z_{s,eff}$ (equation (4)) and finally used to obtain U_{con} for use in equation (9). The results shown in Figures 5 to 7 represent apparent, active and reactive power. In Figure 5, the bonding effect for apparent power is visible as the slope of the curve and the peak values decrease. From this figure, it

**Figure 5.** Apparent power consumption in piezo-impedance transducer.**Figure 6.** Active power consumption in piezo-impedance transducer.

is clear that due to the adhesive bonding, the power required by PZT patch to initiate the structural deformation is obstructed by the presence of the bond.

Similarly, Figure 7 shows the effect of the bond layer on the reactive power. It can be observed that the reactive part of the piezoelectric power (equation (18)), which is the stored charge, is virtually same as apparent power because the imaginary part of admittance is almost of the same magnitude as the absolute value of the complex electromechanical admittance. This indicates the strong reactive nature of electromechanical system. The piezo-coupled reactive power consists of the mechanical reactive power related to the mass (kinetic energy), spring (potential strain energy) and electric reactive power (electric and magnetic field energy of capacitors and inductors).

Power consumed by the PZT patch in terms of heat due to the resistive admittance of the PZT material as well as the losses in the structure is represented by the dissipative power component shown in Figure 6. For the bonding case, the mechanical resistive power is less

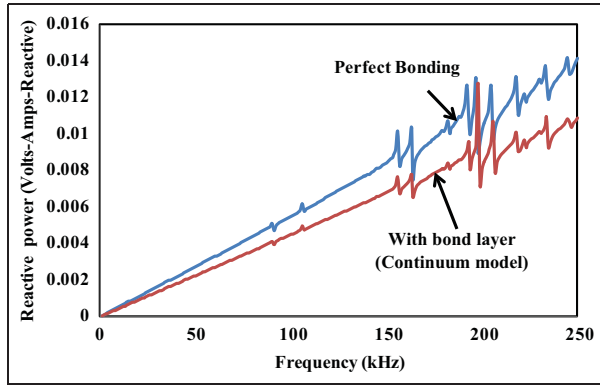


Figure 7. Reactive power consumption in piezo-impedance transducer.

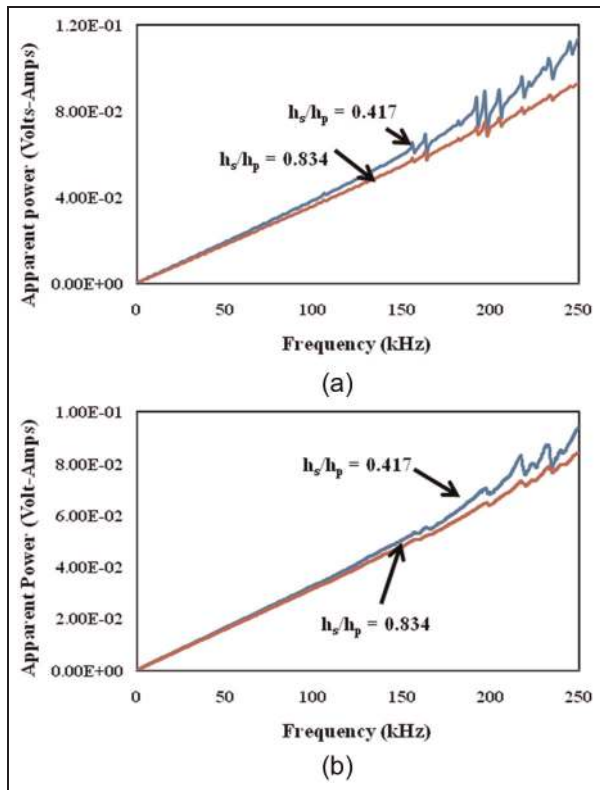


Figure 8. Apparent power consumption for two different bond thickness ratios ($h_s/h_p = 0.417$ and 0.834): (a) analytical signature and (b) experimental signature.

dominant than the perfect bonding case, hence the active energy dissipation for coupled interaction phenomena gets lowered in the presence of the adhesive bond. The phenomenon ultimately indicates that the entire process is mechanically more reactive because more energy is stored in the PZT patch itself.

The experimental investigation of power component has been studied for two different bond thickness ratios ($h_s/h_p = 0.417$ and 0.834) for the same aluminium block shown in Figure 4 (Bhalla and Soh, 2004b). Figures 8 to 10 represent the experimental apparent,

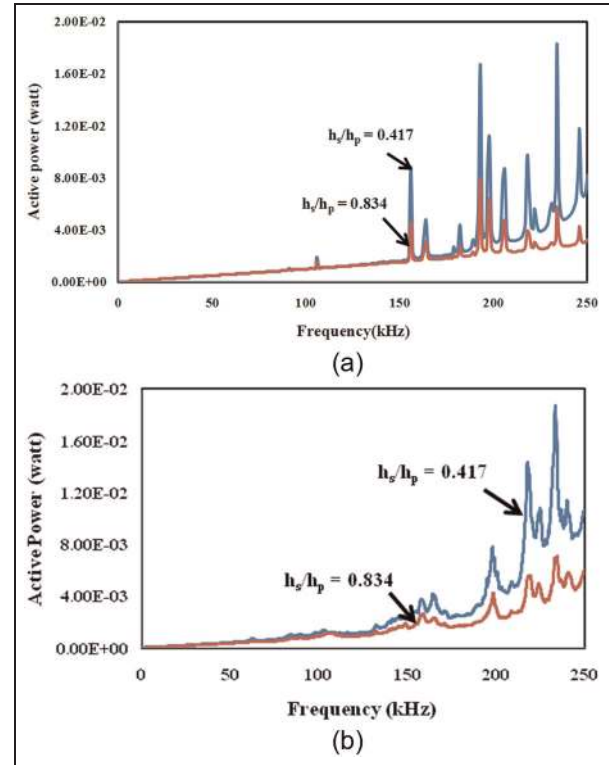


Figure 9. Active power consumption for two different bond thickness ratios ($h_s/h_p = 0.417$ and 0.834): (a) analytical signature and (b) experimental signature.

active and reactive power components with corresponding analytical results based on the continuum model for different bond thickness ratio. As evident from these figures, the bonding effect on various power components measured through the experiments exhibits similar trend as the analytical power component does. For higher bond thickness ratio, the apparent, reactive and active power values are reduced.

The power rating (the maximum power over the frequency range that piezo-patch is expected to operate) is compared in Figure 11(a) for three different models – the perfect bond, the refined model (Bhalla and Moharana, 2013) and the continuum model (Moharana and Bhalla, 2014). Figure 11(b) shows the experimental power rating of piezo-active system with two different types of bond thickness ($h_s/h_p = 0.417$ and 0.834) using continuum-based shear lag model. It is clearly evident that the analytical power requirement is very close to the experimental values because of the higher accuracy of continuum approach. The adhesively bonded PZT patch has lesser power rating than the idealized perfect bond situation. The continuum model predicts marginally higher power rating than the refined model. The piezoelectric materials have an electromechanical efficiency which indicates the energy transfer rate between the stored strain and the electrical energy; however, it is only a material index and cannot be used to evaluate the effectiveness of piezoelectric actuators integrated in a mechanical material system.

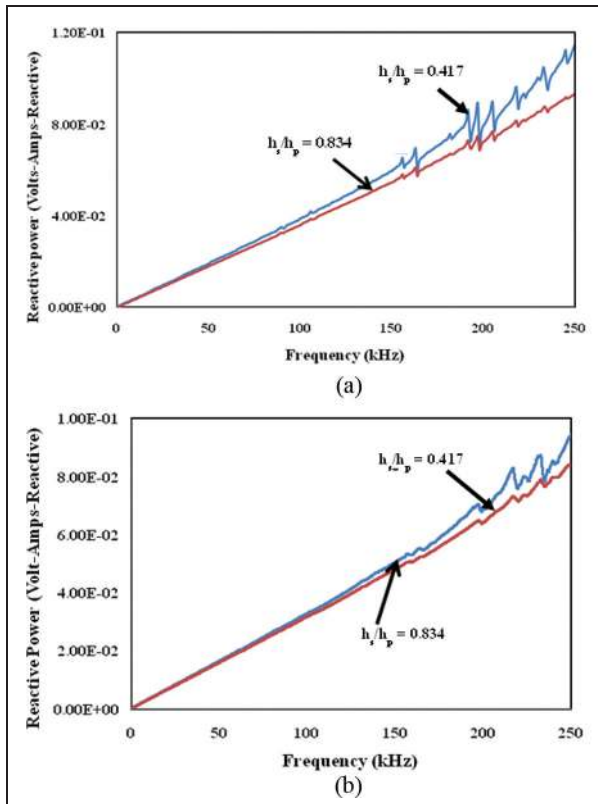


Figure 10. Reactive power consumption for two different bond thickness ratios ($h_s/h_p = 0.417$ and 0.834): (a) analytical signature and (b) experimental signature.

From Figure 12, it is clearly observed that lower power is dissipated (lowered resonance peak) for adhesive bonded case because additional losses (due to adhesive bonding) occur along with other conventional loss (heat, sound and electrical energy).

The power factor in the electrical theory is defined as the ratio of the dissipative power to the supplied (or apparent) power. The power factor of an electrical system represents the capability of the electrical network to convert the supplied electrical energy into heat, light or mechanical energy. In the case of the PZT patch in the EMI technique, we can physically interpret the power factor as the efficiency or effectiveness of the piezo-patch to induce the mechanical response of the structure. The power factor of the piezo-driven system can be defined as (Liang et al., 1994)

$$\cos \phi = \frac{W_D}{W_A} = \frac{\text{Re}(\bar{Y}|_{\delta=0, \eta=0})}{|\bar{Y}|} = \frac{G_{(\delta=\eta=0)}}{|Y|} \quad (21)$$

The system efficiency defined by equation (21) is used to evaluate the amount of the energy dissipated due to the structural damping, that is, the effectiveness of the PZT patch to excite the mechanical system, as graphically presented in Figure 12. The adhesively bonded PZT patch has lower power factor than idealized

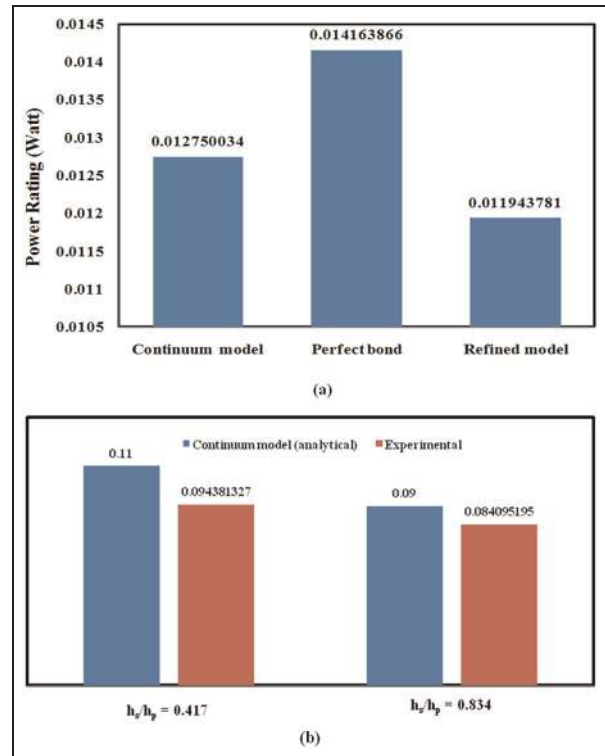


Figure 11. (a) Comparison of maximum power requirement for piezo-structure interaction models and (b) power rating for two different bond thickness ratios ($h_s/h_p = 0.417$ and 0.834). PZT: lead zirconate titanate.

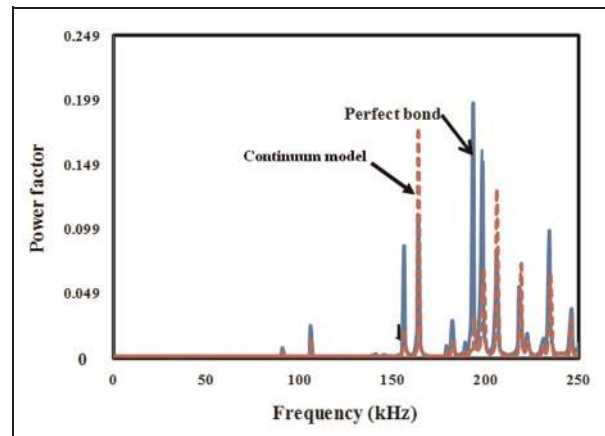


Figure 12. The efficiency of PZT patch to excite the piezo-active system.

perfectly bonded patch. The height of a resonance peak indicates the effectiveness of the patch to excite that particular mode. For the bonding case, the peak and the slope of the curve have been lowered as compared to perfect bond, which indicates that the overall efficiency of PZT patch degrades in the presence the bond. The transducer efficiency is an important parameter in the optimal design of actuator configuration (actuator impedance) and location.

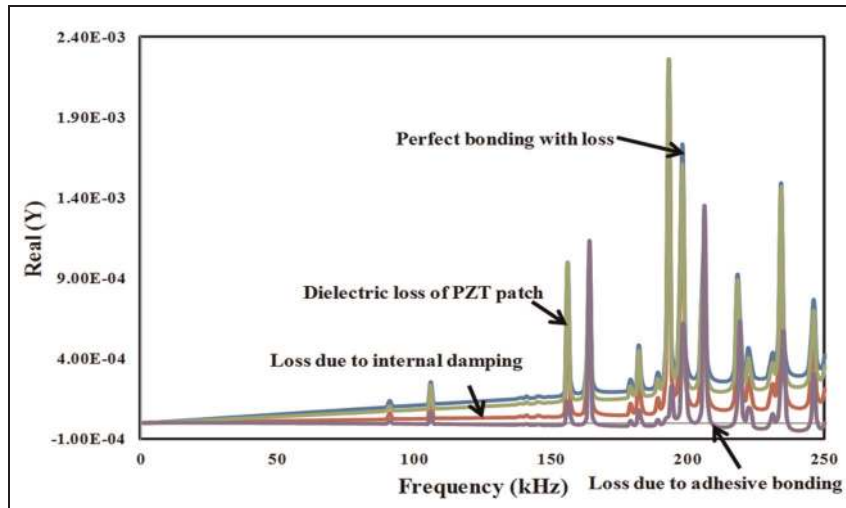


Figure 13. The real part of coupled signature illustrating how active component of electrical power is consumed in electromechanical interaction process.

PZT: lead zirconate titanate.

Figure 13 illustrates how the power supplied to the system is consumed, represented by the real part of admittance (see equation (9)). The real admittance comprised four distinct components illustrated in Figure 13. The first (I) plot results from the perfect bonding case. This is achieved by assuming that there is (1) no adhesive bond between the PZT patch and host structure, (2) zero mechanical damping and dielectric loss ($\delta = \eta = 0$) for the PZT patch and (3) absence of shear lag mechanism. The second (II) plot results from the mechanical loss, which is calculated by assuming zero dielectric loss for the PZT patch ($\eta \neq 0, \delta = 0$) for the perfect bonding case. The third (III) curve is obtained for the dielectric loss, estimated by assuming zero internal damping for ($\eta = 0, \delta \neq 0$) the perfect bonding case. The fourth (IV) plot is obtained by accounting for the shear lag effect calculated by assuming zero mechanical ($\eta = 0$) and dielectric loss ($\delta = 0$) for PZT patch, but considering the patch to be adhesively bonded (loss due to bonding is duly considered).

Energy conversion efficiency of piezo-active mechanical system

The energy consumption and requirements are fundamental concerns for the viability of piezo-active systems for various applications which are weight and volume sensitive, such as noise control of aircraft cabins, submarine quietening and the EMI technique for SHM. The energy conversion factor represents the efficiency of the PZT patch for energy conversion from the electrical to the mechanical domain. When a PZT patch is integrated with an active mechanical system, energy conversion efficiency factor is required to estimate the usefulness of the piezo-active system, which in turn depends upon the mechanical damping, intermolecular bonding between

the PZT patch and structure (characteristic of adhesive bond), structural stiffness, piezoelectric properties of the patch and the imposed boundary conditions.

Liang et al. (1994) determined the power and energy variation using 1D EMI model to design an efficient intelligent structure and illustrated its optimized performance in real-life applications by studying the different components of power (reactive, dissipative) and power efficiency relationship. They demonstrated numerically and experimentally that the total energy flow in the system produced conversational phenomena of electrical and thermal energy within the system. They predicted that in the electromechanical coupling system, it is the strain energy (which is reactive in nature) which interacts with the system (converse effect, acts as actuator) and is consumed in the various mechanical phenomena (damage, failure and thermal loss) in the region of resonance peak. The overused strain energy is converted to electrical energy (direct effect, as sensor) and manifests as the coupled admittance signature. The drawback of this model is that it does not account for the energy losses due to shear lag effect, besides being restricted to 1D. Hence, power output is over estimated.

The energy dissipation within a PZT patch results from mechanical loss and electrical loss. The modelling of these dissipations in the frequency domain analysis is usually conducted by using complex elastic modulus $\overline{Y}^E = Y^E(1 + \eta j)$ and complex electrical permittivity $\overline{\epsilon}_{33}^T = \epsilon_{33}^T(1 - \delta j)$. Some studies (Bondarenko et al., 1982; Martin, 1974) suggest a third source of energy dissipation resulting from the 'imperfection of energy conversion', which is depicted by the hysteresis between the applied electrical field and induced strain. The energy conversion within a PZT patch involves the conversion of electrical energy to mechanical potential and kinetic energy and electrical energy to heat (dissipation).

Later on, Liang et al. (1996) made an investigation for specifically coupled mechanical and electrical performance and derived a working index for the piezo-impedance model. Liang and co-workers mainly focused on the methodology and its utilization in various applicable fields such as optimal actuator location, modal analysis and acoustic power prediction. In a different publication (Liang et al., 1995), a simplified actuator power factor (ψ) was derived to obtain the structural response for changing actuator location and configuration, expressed as

$$\psi = \frac{2\pi\eta K_M y^2}{K_E V E^2} \quad (22)$$

where η is the mechanical loss factor of structure, y is the structural response and E refers to applied electric field. K_M and K_E are the proportionality factors for total mechanical and electrical energy and V is the actuator volume. They concluded that the optimized actuator power factor is more useful to obtain the structural response for a different actuator location. The optimized actuator power factor is also applicable for experimentation and system optimization of an active control model. However, the above studies disregarded the presence of the bond layer. In the following sections, we present analysis considering the bond layer.

Sirohi and Chopra (2000a, 2000b) determined the power consumption of piezo-active system for surface-bonded and free PZT patch experimentally, duly considering the non-linear variation of dielectric permittivity (ϵ_{33}^T) and dissipation factor ($\tan \delta$) for a particular electric field. Once the complex electromechanical admittance is calculated, the voltage drawn and current flow for an active piezo-system can be easily estimated. They introduced the shear lag correction for strain (ϵ_1) voltage relationship by introducing effective sensing length (K_b), expressed as

$$\epsilon_1 = \frac{V_0}{K_b K_p S_q^*} \quad (23)$$

where K_p and K_b are the correction factors to be taken into account for shear lag and Poisson's ratio. S_q^* is the circuit sensitivity and V_0 is the peak excitation voltage. The next section carries the analysis for bond layer.

Energy conversion efficiency ratio for bonding influence on piezo-impedance system

The energy conversion efficiency (λ) can be defined as the ratio of the total energy used for mechanical response (from the piezoelectric induced strain) to the total energy supplied to the system during the piezo-mechanical interaction phenomena. Mathematically, it can be expressed as (Liang et al., 1995)

$$\lambda = \frac{E_{usede}}{E_{supplied}} \quad (24)$$

The above ratio represents the inside direction of flow of physical energy. Therefore, in dynamic applications, the electrical energy and the power will be averaged under each cycle of alternating current. The energy lost per cycle will be in the form of dissipative and reactive energy, according to which, the loss ratio can be divided into two categories. The first term is the *piezo-dissipative loss ratio*, which is concerned with dissipative power (loss due to heat, sound, structural damping and dielectric loss) and can be defined as (Liang et al., 1996)

$$\lambda_{PZT-str} = \frac{E_{mechanically-dissipative}}{E_{total-dissipation}} = \frac{\text{Re}(P_m)}{W_D} = \frac{G_{(\delta \rightarrow 0)}}{G} \quad (25)$$

where P_m is the mechanical power, which can be computed as $\bar{Y}_{\delta \rightarrow 0}$. The second term is the *piezo-reactive loss ratio* resulting due to electrically reactive nature of the piezo-capacitance, which always has tendency to store energy in the system temporarily. So, it represents the instantaneous energy conversion factor of the dynamic piezo-structure system and can be formulated as

$$\lambda_{PZT-elec} = \frac{E_{mechanically-reactive}}{E_{total-reactive}} = \frac{\text{Im}(P_m)}{W_R + \text{Im}(P_m)} \quad (26)$$

Again, the average energy dissipated and converted per cycle is considered for the dynamic case. Investigating power conversion will also provide information on the direction of the energy flow in piezo-active system. The energy conversion efficiency ratio defined by equations (25) and (26) is obtained for both perfect bonding and adhesive bonding case. Figure 14 compares the dissipative loss ratio for the piezo-active model for perfect bonding and adhesive bonding case. Again, the continuum model has been used for the adhesive bonding case. The plot has been restricted to first two natural frequency range (91 and 106 kHz) for

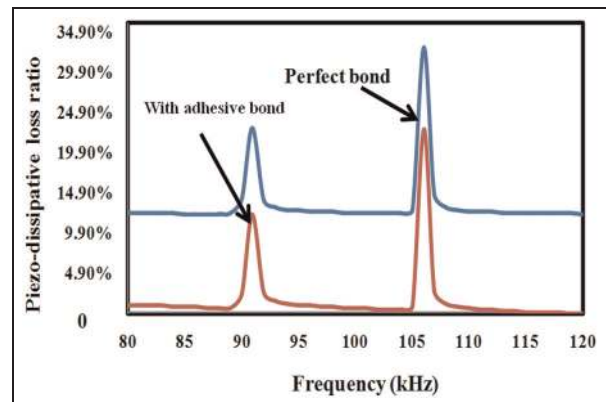


Figure 14. Dissipative energy conversion efficiency ratio for integrated piezo-structural model.

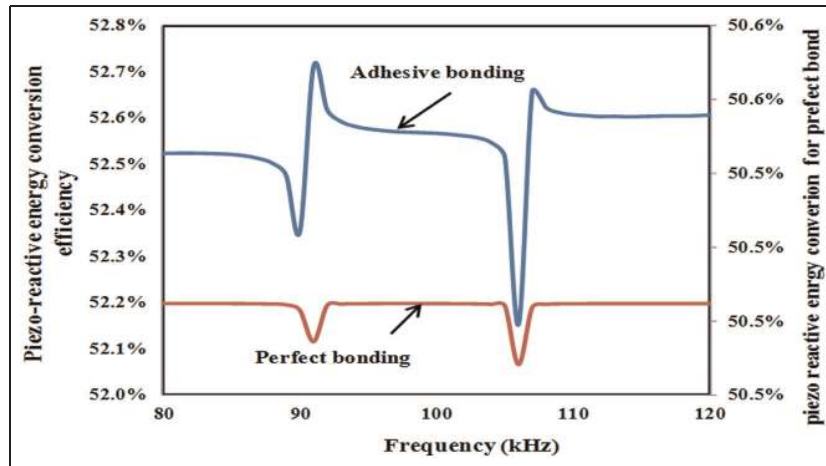


Figure 15. Reactive energy conversion efficiency ratio for integrated piezo-structural model.

greater clarity. From this figure, it can be observed that for the bonding case, the loss ratio has been low, that is, lesser energy is dissipated in the form of heat, sound and damping in the presence of the adhesive bond, indicating less efficient piezo-structural interaction. Figure 15 similarly shows the plot for the reactive loss efficiency ratio. In the frequency range considered (91 and 106 kHz), the reactive energy conversion efficiency is lesser for perfect bonding. There is an increase in the efficiency for the bonding case. The reactive energy conversion efficiency ratio given by equation (26) indicates the instantaneous energy conversion and represents the real coupled interaction phenomena within the PZT patch for any dynamic application. As apparent from Figure 15, the reactive mechanical energy is thus significantly higher for adhesively bonded PZT patch as compared to the perfect bonding case.

Formulation of modified electromechanical coupling coefficient

The electromechanical property is the process of phase transformation of crystals from ferroelectric to paraelectric phase, famously known as the morphic effect. It is an indicator of the effectiveness of the piezo-patch to convert the electrical energy to mechanical energy and vice versa. Theoretically, the electromechanical coupling coefficient can be expressed as (Ikeda, 1990)

$$K_{eff}^2 = \frac{\text{Mechanical energy converted due to piezo deformation}}{\text{Total electrical energy input}} \quad (27)$$

It can be seen that at lower frequency range, the force transfer phenomenon is accelerated to 50%–70% as reported by Liang et al. (1996), so that the energy delivered from one form to other form is greatly enhanced. For this reason, the higher value of k_{eff}^2 at

lower frequency range is generally adapted by manufacturers for well-designed piezo-ceramic elements, whose efficiency of conversion can be maximized up to 95%. So, by definition, the electro-mechanical coupling coefficient can be defined as the ratio of the converted, usable energy delivered by the piezo-electric element, to the actual energy supplied for excitation.

k_{eff}^2 is frequently used to express the effective coupling coefficient of an arbitrary resonator. Experimentally, it can be measured from fundamental resonance or at any overtone and can be expressed as (Seacor Piezo Ceramics, 2012)

$$k_{eff}^2 = \frac{f_a^2 - f_r^2}{f_r^2} \quad (28)$$

where f_a and f_r are the frequencies at anti-resonance and resonance points respectively.

The coupling coefficient can be calculated for the various modes of vibration. For SHM, the piezo-mechanical coupling coefficient for 1D excitation (lateral and longitudinal) can be defined as (Mason, 1966)

$$k_{31} = \frac{d_{31}}{\sqrt{\epsilon_{33}^T S_{11}^E}} \quad (29)$$

where $\overline{\epsilon_{33}^T}$ and $\overline{S_{11}^E} = 1/\overline{Y^E}$ are the two complex terms, which can be split into real and imaginary parts. The real part of the conversion factor indicates the capability of a PZT material to convert electrical energy to mechanical energy and vice versa. The imaginary part reflects the energy dissipation and should remain positive according to the sign convention used in a thermodynamic system (Liang et al., 1996). Liang et al. (1995) proposed the modified electromechanical coupling coefficient to take care of all the losses (piezoelectric and mechanical), which is expressed as

$$k_{eff}^2 = \frac{[d_{31}(1 - i\eta_{em})][d_{31}(1 - i\eta_{em}^*)][Y^E(1 + j\eta)]}{[\epsilon_{33}^T(1 - j\delta)]} \quad (30)$$

where η_{em} is the piezo-mechanical loss factor for active system. The approach was improved but not realistic as the force/strain transfer between the PZT patch and the structure through the bond layer has been ignored. They redefined the coupling coefficient introducing a complex piezoelectric constant $d(1 + i\eta_{em})$ to describe the hysteretic behaviour, where η_{em} is the piezo-mechanical loss factor which was measured experimentally as

$$\eta_{em} = 0.034 + 2.92 \times 10^{-5}f \quad (31)$$

where f is the frequency (Hz) and η_{em}^* is the complex conjugate of η_{em} .

The electrical energy input from the piezo-capacitor can be expressed mathematically as

$$E_{elect} = \frac{1}{2}CV^2 \quad (32)$$

where $C = (k_r \epsilon_0 lb)/t$; k_r is the relative dielectric permittivity and ϵ_0 is the electrical permittivity for vacuum. For PZT materials of grade PIC 151 (PI Ceramic, 2010), following values are considered for present derivation

$$k_r = 2400 \text{ and } \epsilon_0 = 8.85 \times 10^{-12} \text{ F/m}$$

Total mechanical energy stored in PZT patch due to piezo-mechanical displacement is given by

$$E_{mech} = \frac{1}{2} \int_V T_1 S_1 dV \quad (33)$$

where T_1 and S_1 are axial stress and strain along x -direction, respectively, and the stress (T_1) can be expressed as

$$T_1 = \overline{Y^E}(S_1 - \Lambda) \quad (34)$$

where free piezoelectric strain $\Lambda = d_{31}E_3$.

Hence, from equations (33) and (34)

$$E_{mech} = A \int_l \left[\overline{Y^E}(S_1 - \Lambda) S_1 \right] dl \quad (35)$$

Now, we can define coupling coefficient (k_{eff}^2) for mechanical to electrical energy conversion as

$$k_{eff}^2 = \frac{A \int_l \left[\overline{Y_{11}^E}(S_1 - \Lambda) S_1 \right] dl}{\frac{1}{2} CV^2} \quad (36)$$

This modified coupling coefficient (k_{eff}^2) is derived with consideration of the energy loss due to shear lag along with all the complex conjugates (dielectric and mechanical loss) of piezo properties and is thus more accurate and realistic than previous model (equation (30); Liang et al., 1996). The value for k_{eff}^2 has been estimated for the conversion of mechanical energy to the electrical energy and vice versa at first natural frequency (91 kHz). For mechanical to electrical energy conversion, the coupling coefficient is found to be 0.1545, and

for electrical to mechanical energy conversion, it is estimated as 6.4737. The value of k_{eff}^2 for mechanical to electrical energy conversion is low because the shear lag phenomena play a significant role due to the presence of adhesive bond.

Conclusion

This article has presented the electrical requirements of the proposed piezo-bond model and investigated its real-life utility and applications in the area of modelling of active piezo-structure interaction. Different components of input power have been determined for adhesive effect using continuum-based modelling approach. For better understanding of the piezo-structure coupled interaction mechanics, various energy conversion efficiency ratios and a new modified electromechanical coupling coefficient have been derived, which further aid in effective understanding of the piezo-elastodynamic model and can facilitate optimum use of PZT patch for various purposes such as activation and damage detection duly considering the bond layer. In general, the presence of the bond layer lowers the active or the useful power consumption of electromechanical systems.

Declaration of conflicting interests

The authors declare that there is no conflict of interest.

Funding

This research received no specific grant from any funding agency in the public, commercial or not-for-profit sectors.

References

- Bailey T and Hubbard JE (1985) Distributed piezoelectric-polymer active vibration control of a cantilever beam. *Journal of Guidance, Control, and Dynamics* 6(5): 605–611.
- Bhalla S and Moharana S (2013) A refined shear lag model for adhesively bonded piezo-impedance structure. *Journal of Intelligent Material Systems and Structures* 24(1): 33–48.
- Bhalla S and Soh CK (2004a) Impedance based modeling for adhesively bonded piezo-transducers. *Journal of Intelligent Material Systems and Structures* 15(12): 955–972.
- Bhalla S and Soh CK (2004b) Structural health monitoring by piezo-impedance transducers I: modelling. *Journal of Aerospace Engineering* 17(4): 154–165.
- Bhalla S and Soh CK (2004c) Structural health monitoring by piezo-impedance transducers II: applications. *Journal of Aerospace Engineering* 17(4): 166–175.
- Bhalla S, Gupta A, Bansal S, et al. (2009) Ultra low cost adaptations of electro-mechanical impedance technique for structural health monitoring. *Journal of Intelligent Material Systems and Structures* 20(8): 991–999.
- Bondarenko AA, Karas NI and Ulitko AF (1982) Methods for determining the vibrational dissipation characteristics of piezoelectric structural elements. Institute of Mechanics, Academy of Sciences of the Ukrainian SSR, Kiev. translated from *PrikladnayaMekh.* (Plenum), 18(2): 104–108.

- Crawley EF and De Luis J (1987) Use of piezoelectric actuators as elements of intelligent structures. *AIAA Journal* 25(10): 1373–1385.
- Dimitriadis EK, Fuller CK and Rogers CA (1989) Piezoelectric actuators for distributed noise and vibration excitation in thin plates. *ASME Failure Prevention and Reliability* 6: 223–233.
- Dugnani R (2009) Dynamic behavior of structure-mounted disk-shape piezoelectric sensors including the adhesive layer. *Journal of Intelligent Material Systems and Structures* 20: 1553–1564.
- Giurgiutiu V and Santoni-Bottai G (2006) Finite element modeling and simulation of piezoelectric wafer active sensors interaction with the host structure for structural health monitoring. In: *SPIE's 13th international symposium on smart structures and materials and 11th international symposium on NDE for health monitoring and diagnostics*, San Diego, CA, 26 February–2 March 2006, #6174-107.
- Giurgiutiu V and Santoni-Bottai G (2009) Extension of the shear-lag solution for structurally attached ultrasonic active sensors. *AIAA Journal* 47(8): 1980–1983.
- Han L, Wang XD and Sun Y (2008) The effect of bonding layer properties on the dynamic behaviour of surface bonded piezoelectric sensors. *International Journal of Solids and Structures* 45: 5599–5612.
- Huang G, Song F and Wang X (2010) Quantitative modeling of coupled piezo-elasto dynamic behavior of piezoelectric actuators bonded to an elastic medium for structural health monitoring: a review. *Sensors* 10: 3681–3702.
- Ikeda T (1990) *Fundamental of Piezoelectricity*. Oxford: Oxford University Press.
- Jin C and Wang X (2011) Analytical Modelling of the Electromechanical Behaviour of Surface-Bonded Piezoelectric Actuators Including the Adhesive Layer. *Engineering Fracture Mechanics*, (78): 2547–2562.
- Liang C, Sun FP and Rogers CA (1994) Coupled electro-mechanical analysis of adaptive material systems – determination of the actuator power consumption and system energy transfer. *Journal of Intelligent Material Systems and Structures* 5: 12–20.
- Liang C, Sun FP and Rogers CA (1995) Determination of design of optimal actuator location and configuration based on actuator power factor. *Journal of Intelligent Material Systems and Structures* 6(4): 456–464.
- Liang C, Sun FP and Rogers CA (1996) Electro-mechanical impedance modeling of active material system. *Smart Materials and Structures* 5: 171–186.
- Lin B and Giurgiutiu V (2012) Power and energy transduction analysis of piezoelectric wafer active sensors for structural health monitoring. *Structural Health Monitoring* 11(1): 109–121.
- Liu W and Giurgiutiu V (2007) Finite element simulation of piezoelectric wafer active sensors for structural health monitoring with coupled field elements. In: *Proceedings of the 6th international workshop on structural health monitoring*, Stanford, CA, September 11–13, 2007.
- Martin GE (1974) Dielectric, elastic, and piezoelectric losses in piezoelectric materials. In: *Proceedings of the 1974 ultrasonics symposium*, Milwaukee, WI, 11–14 November.
- Mason WP (1966) *Crystal Physics of Interaction Process*. New York: Academic Press.
- Moharana S and Bhalla S (2014) A continuum based modeling approach for adhesively bonded piezo-transducers for EMI technique. *International Journal of Solids and Structures*. 51(6): 1299–1310. DOI: 10.1016/j.ijsolstr.2013.12.022.
- Ong CW, Yang Y, Wong YT, et al. (2002) The effects of adhesive on the electro-mechanical response of a piezoceramic transducer coupled smart system. In: *SPIE international conference on smart materials, structures and systems (ISSS)*, (eds B Dattaguru, S Gopalakrishnan and S Mohan), Bangalore, 12–14 December, pp. 191–197. Microart Multimedia Solutions (Bangalore).
- Park S, Lee JJ, Yun CB, et al. (2008) Electro-mechanical impedance-based wireless structural health monitoring using PCA-data compression and *k*-means clustering algorithms. *Journal of Intelligent Material Systems and Structures* 19: 509–520.
- PI Ceramic (2010) *Product Information Catalogue*. Lindstrabe: PI Ceramic. Available at: <http://www.piceramic.de>
- Seacor Piezo Ceramics (2012) <http://www.seacorpiezo.com>
- Sirohi J and Chopra I (2000a) Fundamental behavior of piezoceramic sheet actuators. *Journal of Intelligent Material Systems and Structures* 11(1): 47–61.
- Sirohi J and Chopra I (2000b) Fundamental understanding of piezoelectric strain sensors. *Journal of Intelligent Material Systems and Structures* 11(4): 246–257.
- Stein SC, Liang C and Rogers CA (1994) Power consumption of piezoelectric actuators driving a simply supported beam considering fluid coupling. *Journal of the Acoustical Society of America* 96(3): 1598–1604.
- Tinoco HA, Serpa AL and Ramos AM (2010) Numerical study of the effects of bonding layer properties on electrical signatures of piezoelectric sensors. *Mecánica Computacional XXIX*: 8391–8409.
- Wang BT and Rogers CA (1991) Laminated plate theory for spatially distributed induced strain actuators. *Journal of Composite Materials* 25(4): 433–452.
- Watkins AJ and Kitcher C (2006) *Electrical Installation and Calculations*. 6th ed. London: Elsevier.
- Xu YG and Liu GR (2002) A modified electro-mechanical impedance model of piezoelectric actuator-sensors for debonding detection of composite patches. *Journal of Intelligent Material Systems and Structures* 13(6): 389–396.
- Yang J, Wang Y and Xu RG (2011) Electro-mechanical analysis of piezoelectric patch bonding to beams. In: *Symposium on piezoelectricity acoustic waves and device applications (SPAWDA)*, Shenzhen, China, 9–11 December, pp. 461–464. New York: IEEE.
- Yang Y, Lim YY and Soh CK (2008) Practical issue related to the application of the electro-mechanical impedance technique in structural civil health monitoring of the structures: II. Numerical verification. *Smart Materials and Structures* 17(3): 1–12.
- Yu S, He S and Li W (2010) Theoretical and experimental studies of beam bimorph piezoelectric power harvesters. *Journal of Mechanics of Materials and Structures* 5(3): 427–445.
- Zhang Y, Xu F, Chen J, et al. (2011) Electromechanical impedance response of a cracked Timoshenko beam. *Sensors* 11: 7285–7301.
- Zhou SW, Liang C and Rogers CA (1996) An impedance-based system modeling approach for induced strain actuator-driven structures. *Journal of Vibration and Acoustics: Transactions of the ASME* 118(3): 323–331.